

# There is a Singularity in the Loss Landscape

Mark Lowell\*

National Geospatial-Intelligence Agency

January 19, 2022

## Abstract

Despite the widespread adoption of neural networks, their training dynamics remain poorly understood. We show experimentally that as the size of the dataset increases, a point forms where the magnitude of the gradient of the loss becomes unbounded. Gradient descent rapidly brings the network close to this singularity in parameter space, and further training takes place near it. This singularity explains a variety of phenomena recently observed in the Hessian of neural network loss functions, such as training on the edge of stability and the concentration of the gradient in a top subspace. Once the network approaches the singularity, the top subspace contributes little to learning, even though it constitutes the majority of the gradient.

## 1 Introduction

Despite neural networks' enormous empirical success, the underlying reasons behind their superior generalization remain mysterious. Deep networks have enough capacity to express functions that perfectly match a training set while being perfectly wrong on a test set [26], but do not land on those functions when trained in practice. This implies that the training process plays a role in why deep networks generalize so well.

Neural network training is usually analyzed as a dynamical system [13]. We think of the space of possible network parameters as a landscape, where the height at a point  $\theta$  is the training loss  $\tilde{\mathcal{L}}(\theta)$ . During training the network is rolling downhill, following the gradient of the loss. Because we cannot solve the dynamical system  $\frac{d\theta}{dt} = -\nabla_{\theta}\tilde{\mathcal{L}}(\theta)$  exactly, we discretize the process into steps. At each step, we move in the direction  $-\nabla_{\theta}\tilde{\mathcal{L}}(\theta)$ , with the length of our step proportional to a learning rate  $\eta$ . Provided that  $\eta$  is small enough, this procedure should be a good approximation of the exact solution to the dynamical system.

---

\*Mark.C.Lowell@nga.mil

Recent work, however, has called this interpretation into question. The maximum stable learning rate, which we denote  $\eta^*$ , is determined by the curvature of the loss landscape. If the learning rate  $\eta$  equals or exceeds  $\eta^*$ , then our step overshoots; conceptually, we jump to the other side of a valley instead of rolling down into its interior. [2] showed experimentally that, during training, the curvature rises until  $\eta \approx \eta^*$ , *regardless of the choice of  $\eta$* , which they called training on the **edge of stability**. If training is on the edge of stability, then it no longer approximates the solution of the dynamical system. The optimization process is instead a difference system; the network is bouncing from point to point on the landscape, instead of rolling smoothly downhill.

In this work, we show experimentally that training on the edge of stability is caused by a singularity that forms in the loss as the size of the dataset increases. A submanifold emerges near which  $\|\nabla_{\theta} \tilde{\mathcal{L}}(\theta)\|_2$  is unbounded. The network is attracted to this singularity during training, and subsequent training takes place near its surface. This singularity explains a variety of recently observed phenomena such as training on the edge of stability seen in [2] and the concentration of the gradient in a top subspace seen in [5].

We make four novel claims:

- Neural network training is on the edge of stability across  $n_c - 1$  eigenvectors, not just 1 eigenvector, where  $n_c$  is the number of classes in the dataset.
- The network enters the edge of stability simultaneously with the gradient concentrating in the top subspace.
- Once the network enters the edge of stability, further reduction in the training loss comes from the smaller bulk component of the gradient, not the top.
- All of these phenomena are caused by the network encountering a singularity in the training loss that forms as the size of the dataset asymptotes to infinity.

In Section 2, we review related work on the Hessian of the training loss and modeling training as a dynamical system. In Section 3, we describe our methodology, including how we calculate  $\eta^*$  and the eigenvalues and eigenvectors. In Section 4, we describe the experiments we conducted. In Section 5, we show the results of these experiments. In Section 6, we discuss implications of our results. In Section 7, we review and describe directions for future research.

Code will be released.

## 2 Related Work

The Hessian of the training loss has been studied for some time for its connections to both optimization and generalization. Modern empirical exploration of the Hessian begins with [18] and [19], which showed that the eigenvalues of

the Hessian matrix tends to separate during training into a few high-magnitude top eigenvalues and a larger set of lower-magnitude bulk eigenvalues, but their experiments were limited to shallow networks. [15] and [16] extended this work to deep networks of meaningful capacity. [5] showed that the gradients of the network tend to concentrate in a top component corresponding to those top eigenvalues, which consist of the top  $n_c$  eigenvectors of the Hessian matrix, where  $n_c$  is the number of classes. The authors concluded that this implies that learning happens within a low-dimensional subspace of the parameter space. Finally, [2] showed that, in non-stochastic gradient descent, the top eigenvalue rises until the learning rate approximately equals the maximum learning rate, regardless of the value of the learning rate. They showed that this occurred for a commendably wide array of network architectures, activation functions, loss functions, tasks, and other hyperparameters. However, they showed only that this phenomenon occurred on the single largest eigenvector, and they did not connect it to the existence of a singularity.

On the theoretical side, there have been many attempts to incorporate training dynamics into a theory of generalization [13]. It is common in these works to take the limit as the width of the network approaches infinity and study the resulting system through mean field theory. The Neural Tangent Kernel (NTK), probably the most successful of these approaches, is based on interpreting the infinite-width limit of the network as a kernel function [7]. NTK has been successfully extended to convolutional networks [20], recurrent networks [1], networks with skip connections [12], and generative adversarial networks [4]. However, the NTK scales only the width of the networks, and assumes the other parameters are fixed.

## 3 Methodology

### 3.1 Defining a Singularity

The term “singularity” is somewhat overloaded. Within the neural network literature, it has been used to refer to a region where the Hessian matrix becomes singular, for example [18], or where the Jacobian of the network outputs becomes degenerate, as in [14]. In mathematics, it often refers to a point where the function is non-differentiable. For clarity, in this paper, we define a singularity as:

**Definition 3.1.** *A **singularity** of a function  $F : U \rightarrow V$  is a point  $p \in U$  such that, for any real numbers  $\epsilon, M > 0$ , there exists a point  $p' \in U$  such that  $\|p - p'\|_2 < \epsilon$  and  $\|\nabla F(p')\|_2 > M$ .*

This definition excludes the fold in a ReLU activation, but would include a vertical cusp such as  $x = 0$  for  $F(x) = |x|^{1/2}$ .

### 3.2 The Role of the Hessian Matrix in Training

Suppose there is a space  $\mathcal{X}$  of data points and a space  $\mathcal{Y}$  of labels, with a label function  $u : \mathcal{X} \rightarrow \mathcal{Y}$ . For example,  $x \in \mathcal{X}$  might be images, and  $u(x) = y \in \mathcal{Y}$  might be the category “cat,” “dog,” and so on. We have no direct access to  $u$ , but we are given a finite training dataset of pairs  $\mathcal{T} = \{(x_1, y_1), (x_2, y_2), \dots\}$ , where  $u(x_j) = y_j$ . We wish to use  $\mathcal{T}$  to find a function  $f : \mathcal{X} \rightarrow \mathcal{Y}$  so that  $f(x) = u(x)$  even for  $x$  not found in  $\mathcal{T}$ .

We parameterize  $f$  by a neural network  $f(x, \theta)$ , where  $\theta$  is the vector of network weights. We define  $l(x, y, \theta)$  to be a criterion measuring the difference between the prediction  $f(x, \theta)$  and the label  $y = u(x)$ . The most commonly used criterion is the softmax-cross-entropy loss:

$$l_{ce}(x, y, \theta) = -\log \left( \frac{\exp(f(x, \theta))_y}{\sum_c \exp(f(x, \theta))_c} \right)$$

where  $c$  indexes the outputs of  $f$ . We define the training loss  $\tilde{\mathcal{L}}(\theta)$  as the expectation of the criterion over the training dataset:

$$\tilde{\mathcal{L}}(\theta) = \mathbb{E}_{(x, y) \sim \mathcal{T}} l(x, y, \theta)$$

where, by abuse of notation, we use  $\mathcal{T}$  to denote a random sampling from the dataset  $\mathcal{T}$ . Then, given a change in the weights  $\Delta\theta$ , the order-2 Taylor approximation of the change in the training loss is:

$$\tilde{\mathcal{L}}(\theta + \Delta\theta) - \tilde{\mathcal{L}}(\theta) = \Delta\theta \cdot g_\theta + \frac{1}{2} \Delta\theta^T H_\theta \Delta\theta + \mathcal{O}(\|\Delta\theta\|^3)$$

where  $g_\theta = \nabla_\theta \tilde{\mathcal{L}}(\theta)$  is the gradient of the training loss  $\tilde{\mathcal{L}}(\theta)$ ,  $H_\theta$  is the Hessian matrix of  $\tilde{\mathcal{L}}(\theta)$ , and  $\mathcal{O}(\|\Delta\theta\|^3)$  is an error term. In the case of non-stochastic gradient descent without momentum, we have  $\Delta\theta = -\eta g_\theta$ , where  $\eta \in \mathbb{R}$  is the learning rate. The above equation then becomes:

$$\tilde{\mathcal{L}}(\theta + \Delta\theta) - \tilde{\mathcal{L}}(\theta) = -\eta \|g_\theta\|_2^2 + \frac{1}{2} \eta^2 g_\theta^T H_\theta g_\theta + \mathcal{O}(\eta^3)$$

Because the Hessian matrix is symmetric, its eigenvalues  $\lambda_i$  are all real and it has an orthonormal basis of eigenvectors  $h_i$ , where  $i$  indexes the parameters in  $\theta$ . We order  $\lambda_i$  such that  $\lambda_0 \geq \lambda_1 \geq \lambda_2 \geq \dots$ . If we parameterize  $g_\theta$  in terms of the basis  $h_i$  with coordinates  $d_i$ ,  $g_\theta = \sum_i d_i h_i$ , then  $H_\theta g_\theta = \sum_i \lambda_i d_i h_i$ , and the above equation becomes:

$$\tilde{\mathcal{L}}(\theta + \Delta\theta) - \tilde{\mathcal{L}}(\theta) = \eta \sum_i d_i^2 \left( \frac{1}{2} \eta \lambda_i - 1 \right) + \mathcal{O}(\eta^3)$$

Then, for every eigenvalue  $\lambda_i$ , from [11] we have a corresponding maximum learning rate:

$$\eta_i^* = \frac{2}{\lambda_i}$$

$$\eta^* = \min \eta_i^*$$

In practice  $\mathcal{O}(\eta^3)$  is small enough that it can be neglected, so that we are guaranteed  $\tilde{\mathcal{L}}(\theta + \Delta\theta) < \tilde{\mathcal{L}}(\theta)$  if  $\eta < \eta^*$ . If  $\eta > \eta^*$ , then the change in the loss cannot be predicted, but usually increases. For any eigenvector  $h_i$  such that  $\eta \approx \eta_i^*$ , we say that the gradient is on the **edge of stability** along  $h_i$ . To ease comparisons between networks trained with different  $\eta$ , we define  $\rho_i = \eta/\eta_i^*$ .

To return to our landscape metaphor, at every moment in training,  $\lambda_i$  is proportional to the curvature in the direction  $h_i$ . If we separate our step  $\Delta\theta$  into its components in each direction  $h_i$ , then if  $\rho_i \ll 1$ , the component of our motion in the direction  $h_i$  is carrying us smoothly downhill. If  $\rho_i \approx 1$ , we are landing on the opposite side of a valley, at the same elevation that we started at, making no progress. If  $\rho_i \gg 1$ , then we are landing on the opposite side of the valley at a *higher* elevation, making our loss worse.

We refer to the subspace spanned by the largest  $n_c - 1$  eigenvectors, where  $n_c$  is the number of classes, as the **top subspace**. We refer to the subspace spanned by the remaining eigenvectors, orthogonal to the top subspace, as the **bulk subspace**. Our terminology differs slightly from [5], where the top subspace is the space spanned by the top  $n_c$  eigenvectors. We define  $P_{\text{top}}v$  to be the projection of a vector  $v$  onto the top subspace, and  $P_{\text{bulk}}v$  to be the projection onto the bulk subspace.

### 3.3 Calculating the Eigenvalues

Because neural networks typically have millions of parameters, the Hessian matrix cannot be explicitly calculated. Instead, we obtain Hessian-vector products using the PyTorch autograd engine [17], and find the largest  $k$  eigenvalues and associated eigenvectors using the power iteration method [24]. The power iteration method returns the  $k$  largest eigenvalues by absolute value. However, in practice, we find that the positive eigenvalues invariably have greater magnitude than the negative eigenvalues in the Hessian of the training loss.

## 4 Experiments

We perform all of our experiments using the CIFAR-10 training dataset [9], a set of 50,000  $32 \times 32$  images in 10 classes. We initialize all networks with the Kaiming initialization [6] and train them using non-stochastic gradient descent without momentum.

### 4.1 Exploring the Edge of Stability

We begin by training a large number of networks with a variety of hyperparameters to explore the edge of stability. We train AlexNets [10] and non-normalized VGG-16s [21] with ReLU and tanh activation functions, using a selection of learning rates  $\{0.003, 0.001, 0.0003, 0.0001\}$ . We train the networks until the

training loss drops below 0.1 or we reach  $40\eta^{-1}$  iterations. Every  $\eta^{-1}$  iterations, we pause training and collect a variety of telemetry:

- We calculate the largest 20 eigenvalues  $\lambda_i$  and eigenvectors  $h_i$ , and use them to calculate the maximum learning rates  $\eta_1^*, \dots, \eta_{20}^*$  and the ratios  $\rho_1, \dots, \rho_{20}$ .
- We calculate the training gradient  $g_\theta$  and use the eigenvectors  $h_i$  to calculate its projections  $P_{\text{top}}g_\theta$  and  $P_{\text{bulk}}g_\theta$ .
- Using these projections, we calculate the change in the training loss caused by taking a single optimization step in the direction of  $P_{\text{top}}g_\theta$  and  $P_{\text{bulk}}g_\theta$ . We do this by adjusting the weights and recalculating the loss, not by using the Taylor approximation.

Networks trained with the tanh activation at  $\eta = 0.003$  are omitted from our analyses because they failed to converge. The VGG-16-tanh network at  $\eta = 0.0001$  converged so quickly that we had run these analyses only twice before training terminated.

We additionally perform several sub-experiments to explore specific elements of the behavior of the system:

- To determine the effect of the number of classes in the dataset, we train networks where we drop classes in CIFAR-10 to form datasets with 2, 3, or 5 classes.
- To capture the moment the network enters the edge of stability, we train a network where we run our analysis every 10 iterations instead of every  $\eta$  iterations, but only train for 2000 iterations.

We perform these additional experiments using AlexNet networks with ReLU activation at  $\eta = 0.001$ .

## 4.2 Solving the Dynamical System Exactly

In addition to these experiments to explore the edge of stability, we also trained a set of networks where we attempted to solve the dynamical system  $\frac{d\theta}{dt} = -g_\theta$  exactly. We calculated the eigenvalue  $\lambda_1$  at every iteration, and set the learning rate to  $\min(0.001, 0.5/\lambda_1)$ . Since  $\lambda_1$  is the largest eigenvalue, this will ensure that  $\eta$  will always lie well below the edge of stability for all eigenvectors. We pick this value to be less than the optimal value  $\lambda_1^{-1}$  because we are expecting to enter a region where the curvature itself is changing very rapidly. This procedure should ensure that we remain close to the actual exact solution of the gradient flow. We trained a set of AlexNet networks with ReLU and tanh activations on subsets of CIFAR-10 of varying size  $n_D$  using this process.

## 5 Results

### 5.1 The Gradient Is on the Edge of Stability Across $n_c - 1$ Eigenvectors

We plot  $\rho_9$  and  $\rho_{10}$  for our main series of experiments from Section 4.1 in Figure 1. Because  $\rho_i \geq \rho_{i+1}$ ,  $\rho_9$  lower-bounds  $\rho_i$  for the top subspace, and  $\rho_{10}$  upper-bounds  $\rho_i$  for the bulk subspace. For the high learning rate  $\eta = 0.003$ , or close to the end of training,  $\rho_{10}$  may be close to or on the edge of stability. But as we decrease the learning rate,  $\rho_{10}$  falls steadily toward zero.  $\rho_9$  reaches the edge of stability almost instantly no matter how much we shrink  $\eta$ . At our lowest learning rate  $\eta = 0.0001$ , across all of our architectures,  $\rho_{10}$  never exceeds 0.246 at any point, while  $\rho_9$  always reaches at least 0.693.

This implies that the curvature along the direction of  $h_{10}$  and the corresponding maximum learning rate  $\eta_{10}^*$  are independent of  $\eta$ . The curvature along  $h_9$  increases, and the maximum learning rate  $\eta_9^*$  decreases, as we shrink  $\eta$ , meaning that the network lies on the edge of stability on  $h_1, \dots, h_9$ .

We plot the results of our experiments where we varied the number of classes in Figure 2. Once again we see a clear separation between  $\rho_{n_c-1}$  and  $\rho_{n_c}$ , implying that the number of eigenvectors on the edge of stability is consistently  $n_c - 1$ .

### 5.2 Concentration of the Gradient in the Top Subspace Occurs Simultaneously with the Edge of Stability

In Figure 3, we graph the magnitude of the projection of  $g_\theta$  onto the top subspace  $\|P_{\text{top}}g_\theta\|_2$ , along with the magnitude of the projection onto the bulk  $\|P_{\text{bulk}}g_\theta\|_2$ . We observe that the magnitude of the bulk component remains roughly constant with learning rate, while the magnitude of the top component increases as  $\eta$  shrinks.

In Figure 4, we plot the result of the experiment where we ran our analysis every 10 iterations. We observe that the gradient magnitude explodes at the same iteration the eigenvector enters the edge of stability.

### 5.3 Learning Occurs in the Bulk, Not the Top

We show the mean and standard deviation of the change in the training loss caused by a step in the direction of  $P_{\text{top}}g_\theta$  versus a step in the direction of  $P_{\text{bulk}}g_\theta$  in Table 1. We limit our calculations to iterations where the network is indisputably on the edge of stability, as shown by  $\rho_9 > 0.7$ , and we omit combinations of hyperparameters where this left us with fewer than three iterations to use in this calculation. We consistently see that the change in the loss caused by the top component is either positive or very close to 0, while the standard deviation is large. The change caused by the bulk is consistently negative, with low standard deviation.

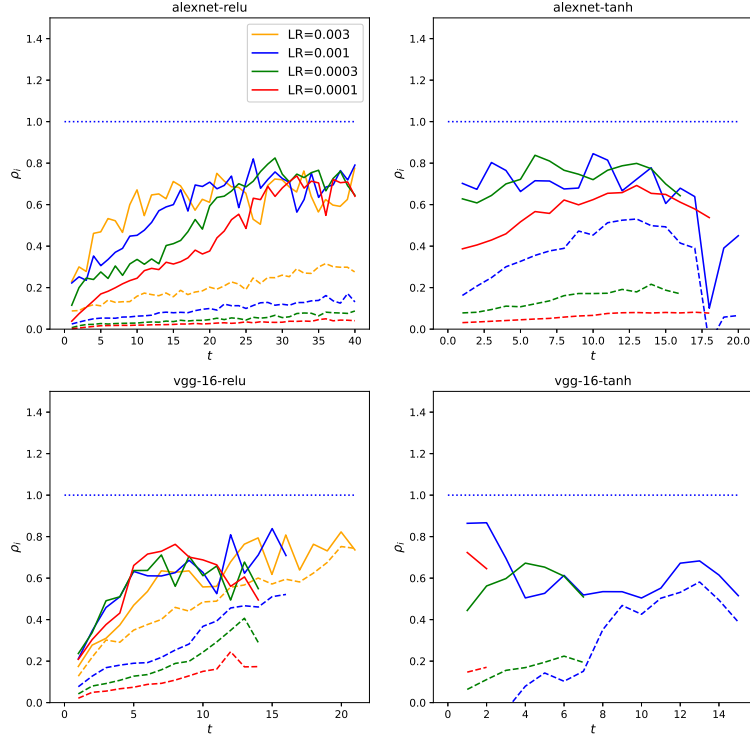


Figure 1: Edge of Stability: The vertical axis represents  $\rho$  while the horizontal axis represents  $t = n\eta$ , where  $n$  is the iteration. Solid curves represent  $\rho_9 = \eta/\eta_9^*$ , while dotted curves represent  $\rho_{10} = \eta/\eta_{10}^*$ . Different colors represent different learning rates, and each subfigure represents a different network architecture and activation function.



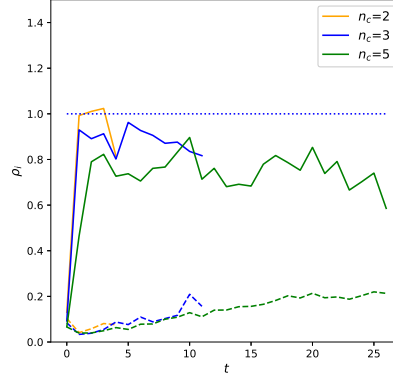


Figure 2: Edge of Stability and  $n_c$ : Solid curves represent  $\rho_{n_c-1} = \eta/\eta_{n_c-1}^*$ , while dotted curves represent  $\rho_{n_c} = \eta/\eta_{n_c}^*$ . Different colors represent different numbers of classes in the dataset. The horizontal axis is  $t = n\eta$ , where  $n$  is the iteration.

$\eta$	Architecture	Mean $\Delta\tilde{\mathcal{L}}$ from $P_{\text{top}}g_\theta$ (std)	Mean $\Delta\tilde{\mathcal{L}}$ from $P_{\text{bulk}}g_\theta$ (std)
0.003	AlexNet-ReLU	0.0043 (0.0172)	-0.0041 (0.0010)
0.001	AlexNet-ReLU	0.0064 (0.0133)	-0.0014 (0.0007)
0.0003	AlexNet-ReLU	-0.0001 (0.0046)	-0.0003 (0.0001)
0.0001	AlexNet-ReLU	-0.0012 (0.0043)	-0.0001 (0.000)
0.001	AlexNet-Tanh	0.0025 (0.0048)	-0.0017 (0.0010)
0.0003	AlexNet-Tanh	0.0007 (0.0031)	-0.0004 (0.0001)
0.003	VGG-16-ReLU	0.0710 (0.0645)	-0.0256 (0.0111)
0.001	VGG-16-ReLU	0.0208 (0.0142)	-0.0072 (0.0035)
0.0001	VGG-16-ReLU	0.0011 (0.0064)	-0.0008 (0.0006)

Table 1: Learning Occurs in the Bulk, not the Top

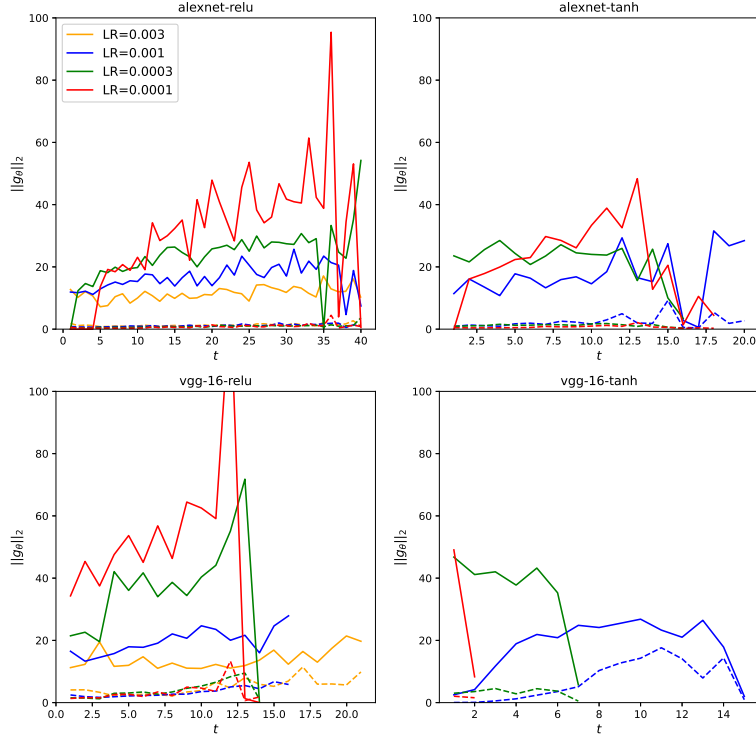


Figure 3: Gradient Concentration: Solid curves represent  $\|P_{\text{top}} g_{\theta}\|_2$ , while dotted curves represent  $\|P_{\text{bulk}} g_{\theta}\|_2$ . Different colors represent different learning rates  $\eta$ . Different subfigures represent different architectures. The horizontal axis is  $t = n\eta$ , where  $n$  is the iteration.

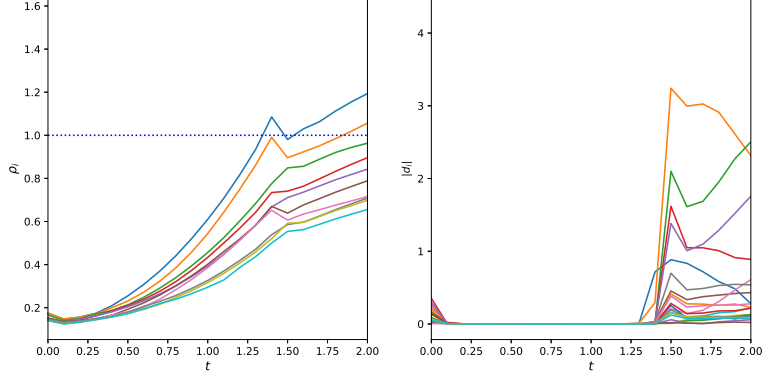


Figure 4: Entering the Edge of Stability: The left subfigure shows  $\rho_1, \dots, \rho_9$ , while the right subfigure shows  $|d_i| = |h_i \cdot g_\theta|$ , for an AlexNet-ReLU trained at  $\eta = 0.001$ . Different colors represent different eigenvalues  $\lambda_i$  and eigenvectors  $d_i$ . The horizontal axis is  $t = n\eta$ , where  $n$  is the iteration.

#### 5.4 The Trajectory of $\theta$ Lies Near a Singularity

The loss landscape does not change when we change  $\eta$ , only the trajectory of  $\theta$  through it. As  $\eta$  decreases, the eigenvalues  $\lambda_1, \dots, \lambda_{n_c-1}$  remain near  $2/\eta$ , while the magnitude of the top component of the gradient  $\|P_{\text{top}}(g_\theta)\|_2$  increases. Suppose we could allow  $\eta$  to reach 0, so that we are solving the dynamical system  $\frac{d\theta}{dt} = -g_\theta$  exactly; this suggests that  $\lambda_1, \dots, \lambda_{n_c-1}$  and  $\|P_{\text{top}}g_\theta\|_2$  would all approach infinity over the course of training. This can occur only if either  $\theta \rightarrow \infty$  or if there exists a point in whose neighborhood  $\|g_\theta\|_2$  is unbounded — in other words, a singularity in  $\tilde{\mathcal{L}}(\theta)$ . In all of our experiments,  $\|\theta\|_2$  increased by much less than 1%, even though we used no regularization, so we can conclude that  $\theta \not\rightarrow \infty$ .

Strictly speaking, the  $\lambda_i, g_\theta$  of a finite-size network with bounded weights trained on a finite dataset must be finite. If we reduced  $\eta$  enough, eventually training would be below the edge of stability. But it is common in theory to make the simplifying assumption that various parameters limit to infinity, for example [7]. If  $n_D = 1$ , so that training is achieved by simply scaling the outputs, then the gradients and curvature are trivial, so we hypothesize that a singularity forms as  $n_D \rightarrow \infty$ .

To test this hypothesis, we attempted to train networks by solving the gradient flow exactly, as discussed in Section 4.2. We plot  $\lambda_1$  versus time for each of these experiments in Figure 5. With ReLU activation, peak  $\lambda_1$  rises linearly with the size of the dataset. A linear regression between the size of the dataset  $n_D$  and peak  $\lambda_1$  has an  $R^2$  of 99.91%. The picture is more complicated with tanh activation, where there is an initial spike in  $\lambda_1$  to a consistent level of about

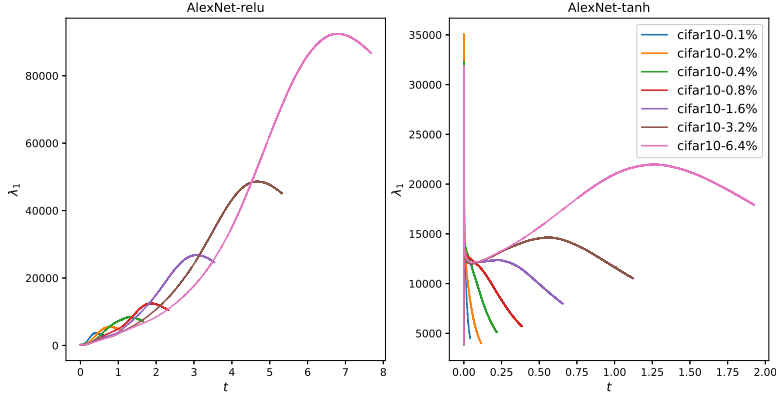


Figure 5: Peak Curvature: Each curve represents  $\lambda_1$  over the course of training an AlexNet on a subset of CIFAR-10, adaptively scaling the learning rate to approximate the exact solution of the differential equations  $\frac{d\theta}{dt} = -g_\theta$ . Different colors represent differently-sized subsets. The left figure uses a ReLU activation, while the right figure uses the tanh activation. The horizontal axis is  $t$ .

30,000, literally one iteration after training begins. For small datasets, this initial spike overwhelms the later peak in  $\lambda_1$  — but we see the peak forming as the dataset size increases, once again rising linearly with dataset size, although at a slower rate than with the ReLU activation.

We saved model snapshots every 100 iterations during training. For our AlexNet-ReLU networks, we reloaded the model weights to the peak curvature, which we denote  $\theta^*$ , and calculated the top eigenvector  $h_1$ . We then sampled a large number of  $\Delta$  between -0.003 and 0.003, adjusted the weights by  $\Delta h_1$ , and calculated the change in the training loss, as shown in the left subfigure of Figure 6. We see a vertical cusp forming as  $n_D \rightarrow \infty$ .

## 6 Discussion

The existence of this singularity has direct implications for understanding generalization in terms of the training process, especially the Neural Tangent Kernel (NTK) [7]. First, this confirms that training *is* a dynamical system, not a difference system. Second, NTK and other mean-field approaches take the limit as the width of the network approaches infinity. Under this assumption, the Hessian of the training loss does not evolve during training. In practice, the scaling of neural networks generally involves scaling the depth, input dimension, and dataset size as well as the width [23][22]. If multiple terms are asymptoting to infinity, then the assumption that the Hessian will not change during training may not hold, as we have shown here.

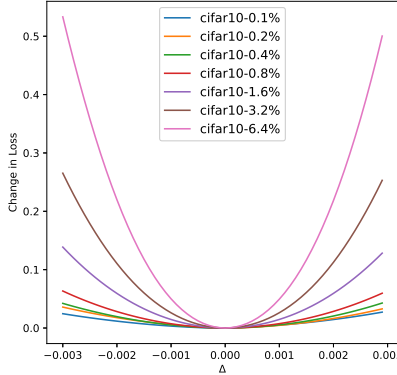


Figure 6: Cusp Formation: Each curve shows the change in  $\tilde{\mathcal{L}}(\theta)$  along the direction  $h_1$  in a neighborhood of the point  $\theta^*$  of peak  $\lambda_1$ . The horizontal axis is the displacement in the direction  $h_1$ , while the vertical axis is the change in the loss,  $\tilde{\mathcal{L}}(\theta^* + \Delta h_1) - \tilde{\mathcal{L}}(\theta^*)$ .

This result also has implications for optimization. There has been considerable interest recently in sharpness-aware optimizers (for example [3]). This result indicates that minimizing sharpness in the top direction is not possible and probably not desirable, while leaving open the possibility that minimizing sharpness in the bulk directions may still be valuable. We might also speculate on a connection to the tendency of adaptive optimizers such as Adam [8] to have lower generalization performance than stochastic gradient descent [25] and to the instabilities that famously plague the training of generative adversarial networks.

## 7 Conclusion

We have shown that, as the size of the dataset increases, a singularity forms in the loss landscape, and training occurs on a trajectory near the surface of the singularity. This singularity causes training to occur on the edge of stability in the top subspace and the gradient in the top subspace to become very large. Despite this, once the network enters the edge of stability, the top component of the gradient contributes very little to improving the loss, with most learning occurring in the bulk component.

In future research, we plan to further explore the connections between the training gradient, the curvature of the loss landscape, and generalization. In particular, decomposing the gradient and the curvature on a layer-by-layer basis is likely a necessary pre-condition for developing a mathematical theory of generalization in deep learning, as is investigating the connection between the training gradient and the *test* gradient.

**Acknowledgements:** This work was supported in part by high-performance computer time and resources from the DoD High Performance Computing Modernization Program.

## References

- [1] Sina Alemohammad, Zichao Wang, Randall Balestrieri, and Richard Baraniuk. The recurrent neural tangent kernel. 2021.
- [2] Jeremy Cohen, Simran Kaur, Yuanzhi Li, J. Zico Kolter, and Ameet Talwalkar. Gradient descent on neural networks typically occurs at the edge of stability. 2021.
- [3] Pierre Foret, Ariel Kleiner, Hossein Mobahi, and Behnam Neyshabur. Sharpness-aware minimization for efficiently improving generalization. 2020.
- [4] Jean-Yves Franceschi, Emmanuel de Bézenac, Ibrahim Ayed, Mickaël Chen, Sylvain Lamprier, and Patrick Gallinari. A neural tangent kernel perspective of GANs. 2021.
- [5] Guy Gur-Ari, Daniel A. Roberts, and Ethan Dyer. Gradient descent happens in a tiny subspace. 2018.
- [6] Kaiming He, Xiangyu Zhang, Shaoqing Ren, and Jian Sun. Delving deep into rectifiers: Surpassing human-level performance on ImageNet classification. 2015.
- [7] Arthur Jacot, Franck Gabriel, and Clément Hongler. Neural tangent kernel: Convergence and generalization in neural networks. 2018.
- [8] Diederik P. Kingma and Jimmy Ba. Adam: A method for stochastic optimization. 2015.
- [9] Alex Krizhevsky. Learning multiple layers of features from tiny images. 2009.
- [10] Alex Krizhevsky, Ilya Sutskever, and Geoffrey E. Hinton. ImageNet classification with deep convolutional neural networks. 25, 2012.
- [11] Yann LeCun, Leon Bottou, Genevieve Orr, and Klaus-Robert Muller. Efficient backprop. *Lecture Notes in Computer Science*, pages 9–50, 1998.
- [12] Yuqing Li, Tao Luo, and Nung Kwan Yip. Towards and understanding of residual networks using neural tangent hierarchy (NTH). 2020.
- [13] Guan-Horng Liu and Evangelos Theodorou. Deep learning theory review: An optimal control and dynamical systems perspective. 2019.

- [14] Eiji Mizutani and Stuart Dreyfus. An analysis on negative curvature induced by singularity in multi-layer neural-network learning. 2010.
- [15] Vardan Papyan. The full spectrum of deepnet hessians at scale: Dynamics with SGD training and sample size. 2018.
- [16] Vardan Papyan. Measurement of three-level hierarchical structure in the outliers in the spectrum of deepnet hessians. 2019.
- [17] Adam Paszke, Sam Gross, Francisco Massa, Adam Lerer, James Bradbury, Gregory Chanan, Trevor Killeen, Zeming Lin, Natalia Gimelshein, Luca Antiga, Alban Desmaison, Andreas Kopf, Edward Yang, Zachary DeVito, Martin Raison, Alykhan Tejani, Sasank Chilamkurthy, Benoit Steiner, Lu Fang, Junjie Bai, and Soumith Chintala. PyTorch: An imperative style, high-performance deep learning library, 2019.
- [18] Levent Sagun, Léon Bottou, and Yann LeCun. Eigenvalues of the hessian in deep learning: Singularity and beyond. 2016.
- [19] Levent Sagun, Utku Evci, V. Uğur Güney, Yann Dauphin, and Léon Bottou. Empirical analysis of the hessian of over-parameterized neural networks. 2018.
- [20] Arora Sanjeev, Simon S. Du, Wei Hu, Zhiyuan Li, Ruslan Salakhutdinov, and Ruosong Wang. On exact computation with an infinitely wide neural net. 2019.
- [21] Karen Simonyan and Andrew Zisserman. Very deep convolutional networks for large-scale image recognition. 2015.
- [22] Chen Sun, Abhinav Shrivastava, Saurabh Singh, and Abhinav Gupta. Revisiting unreasonable effectiveness of data in deep learning era. 2017.
- [23] Mingxing Tan and Quoc V. Le. EfficientNet: Rethinking model scaling for convolutional neural networks. 2019.
- [24] Richard von Mises and Hilda Pollaczek-Geiringer. Praktische verfahren der gleichungsauflösung. *Zeitschrift für Angewandte Mathematik und Mechanik*, 1929.
- [25] Ashia C. Wilson, Rebecca Roelofs, Mitchell Stern, Nathan Srebro, and Benjamin Recht. The marginal value of adaptive gradient methods in machine learning. 30, 2017.
- [26] Chiyuan Zhang, Samy Bengio, Moritz Hardt, Benjamin Recht, and Oriol Vinyals. Understanding deep learning requires rethinking generalization. 2017.